**P2.12     CLIMATOLOGY AND FORECASTING APPLICATIONS FOR ELEVATED THUNDERSTORMS
IN THE GREAT BASIN AND WEST COAST OF THE UNITED STATES**

Alexander Tardy*
NOAA/NWS/Weather Forecast Office, Salt Lake City, Utah

## 1.   INTRODUCTION

Most thunderstorms in the western United States are rooted in the boundary layer and are dependent on surface or near-surface conditions. During the warm season, moist convection increases in coverage and frequency due to the increased instability and periodic moist monsoonal flow. Thunderstorms are most common across the higher terrain of the western United States where air parcels can more easily reach the level of free convection (LFC). Across the valleys and deserts there is often limited low-level moisture and available forcing is not sufficient to lift parcels to the observed high-based LFC. Inversion layers, subsidence and divergent low-level flow can also inhibit or limit convection. There has been recent research (Horgan 2006, Corfidi 2006) which has focused on various aspects of elevated convection such as the severe weather and heavy rainfall threat associated with these events. The research to be presented here utilizes model and observed soundings in an attempt to draw a distinction between elevated moist convection and moist convection which was rooted in the boundary layer across the western United States.

Identifying the potential for elevated thunderstorms and understanding the processes involved poses a significant challenge to operational forecasting. Despite thunderstorms being common during the warm season this convection is typically considered to be terrain-driven and cold pool outflow influenced with a strong diurnal tendency. Given the proper synoptic pattern there can be sufficient mid-level moisture, lift, and elevated deep layer instability to produce thunderstorms which are not dependent on terrain, boundaries or surface diabatic effects. The elevated thunderstorms examined in this study displayed similar intensity whether they occurred nocturnally, over cooler water, in the valleys and deserts, or across the mountainous terrain.

The consequences of these thunderstorm events can have major implications for fire danger, aviation, human activity and agriculture. During a few of these events the intensity of the storms resulted in severe weather. Other elevated thunderstorm outbreaks triggered large and long duration remote wild fires, and in a several cases,

*Corresponding author address:* Alexander Tardy, NWS/WFO, 2242 W. North Temple, Salt Lake City, 84116. email: <alexander.tardy@noaa.gov>

between 2000 and 5000 cloud-to-ground lightning strikes were detected. This climatological study analyzed 86 elevated thunderstorm outbreaks (Table 1) across the western United States using lightning data from the National Lightning Detection Network (NLDN). The study also used composite reanalysis from the Climate Diagnostic Center (CDC) for identifying synoptic patterns (see appendix). Finally, there are forecasting applications presented which use satellite and numerical model data

Prior research on elevated thunderstorms (Colman 1990), demonstrated that the presence of elevated convective available potential energy (defined as ECAPE for this study) was minimal in many events. The thunderstorms in the Colman study were similar to those investigated here since they were isolated from surface diabatic effects and were organized by larger scale dynamics. However, many of the thunderstorms of interest in this study developed in an environment with significant ECAPE. The Colman study further found the elevated thunderstorms to be associated with distinct surface warm fronts that produced a low-level inversion. In the research presented here the frontal structure was often not well defined. The synoptic pattern usually exhibited a relatively dry closed upper low that moved across the eastern Pacific and interacted with a moist air mass that was present or advected into the region (Fig. 1). This has been identified as a typical weather pattern for elevated thunderstorms in the Great Basin and West Coast (Tardy 2001, 2002).

## 2.   EVENT DATABASE AND METHODOLOGY

This climatology of elevated thunderstorms collected events from the period 1999 through 2006 (Table 1) using satellite and lightning data. An event consisted of detected lightning strikes associated with elevated instability on observed soundings. If the observed profile was determined to not be representative of the area of strikes or the time of occurrence then available model data (e.g., RUC and NAM soundings) were used. The distinction between surface-based and elevated moist convection was the primary challenge for establishing the database. Events that occurred during the typical diurnal period with a boundary layer consisting of high static stability (i.e., 2100 to 0800 MDT or PDT) were easier to determine

whether the boundary layer was involved. Many events exhibited little or no daytime convection but had a nocturnal increase in lightning activity. In order to fully understand the process of elevated convection lightning was not a prerequisite for identifying elevated convection (e.g., formation of altocumulus castellanus).

This paper will discuss results from the event database and establish a climatological pattern associated with elevated convection. In addition, it will present a sample of significant events and research findings, as well as identify forecasting challenges and demonstrate applications.

## 3. CLIMATOLOGY OF EVENTS

The cases in this study contained a broad range of thunderstorm events. When all the events (86 cases in Table 1) were compiled in an attempt to identify favored synoptic patterns, distinct similarities emerged. Using composite reanalysis data from CDC illustrated that the common weather pattern for all events in the study was an upper level low pressure area or short-wave trough along the West Coast or in the Great Basin (Figs. 1 through 6). These systems were typically slow moving as they approached the seasonal 4-corners upper ridge and sometimes entered the region as a closed circulation. This pattern has also been identified as critical for fire weather (see link in appendix).

The composite of events in years 1999, 2000 and 2002 (see Figs. 1 and 3) produced a closed contoured low. This is indicative of the large well-defined closed lows that affected the West Coast during those years. In some cases, sufficient mid-level moisture was present, and in other events the disturbance advected moisture into the region.

The analysis of the database also produced a similar atmospheric profile to that depicted in Figure 7. The ingredients typically included either of a dry boundary layer, a stable marine layer, or a radiational inversion. In most cases, there was insufficient low-level lift or substantial convective inhibition (CIN) that would not allow boundary layer air parcels to reach their LFC (no surfaced-based CAPE) with the main exception being across nearby mountains. The nocturnal, over cold water and deep dry valley events made it more apparent that the convection was not rooted in the boundary layer. Steep elevated lapse rates were always present but varied in depth. This variation was important for the strength of the associated updrafts. However, the depth was sometimes altered by synoptic scale layer lifting (i.e., omega) and the presence of dry air in the upper levels.

In addition, the moisture source for the high based convection originated between 700 and 500 mb. Rapid advection of moisture into a region with steep mid-level lapse rates and the dry upper levels (near 400 mb) often resulted in destabilization of the vertical profile. The profile in many events took on an hourglass appearance since moisture was between two dry layers.
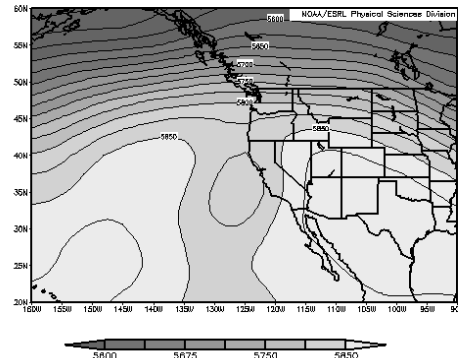


*Fig. 1. Composite reanalysis of 500-mb geopotential heights for events during period 1999 to 2000. Height lines contoured every 25 m.*
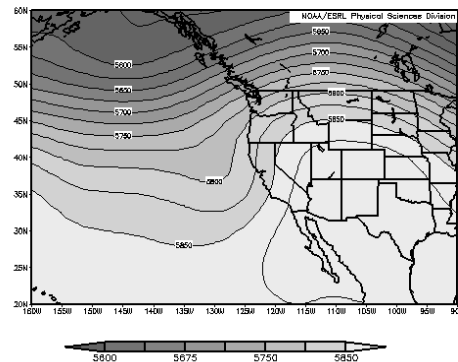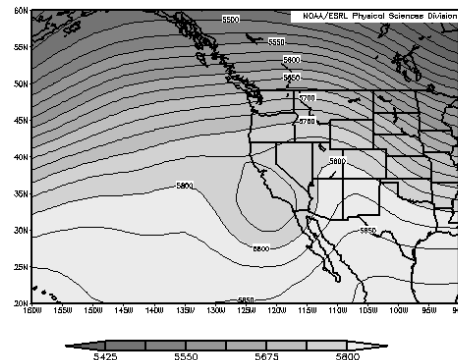


*Fig. 2. Same as Fig. 1 for 2001.*

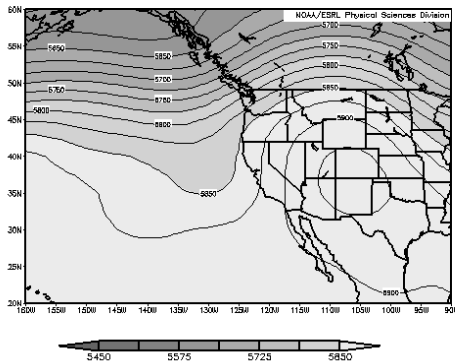

*Fig. 3. Same as Fig. 1 for 2002.*
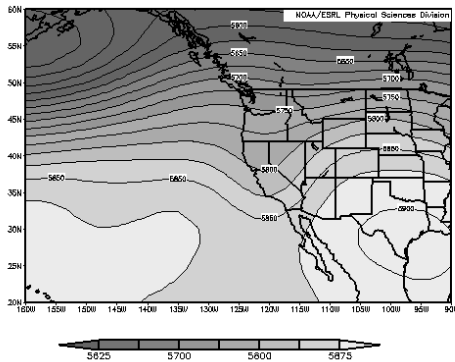
*Fig. 4. Same as Fig. 1 for 2003.*
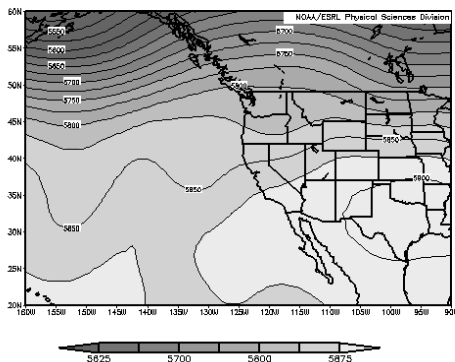


*Fig. 5. Same as Fig. 1 for 2004-05.*



*Fig. 6. Same as Fig. 1 for 2006.*

The identification of these ingredients was key to understanding the potential for elevated convection. However, the prediction and quantification of these ingredients (e.g., omega) remains a challenge for forecasters and numerical weather prediction. Modest variations can result in towering elevated cumulus such as altocumulus castellanus versus widespread deep moist convection and lightning. In some cases, elevated

thunderstorms can transition into daytime surface-based convection as insulation modifies the low-level profile such that surface-based parcels can attain their LFC. More often, elevated convection was observed to increase during the night hours.
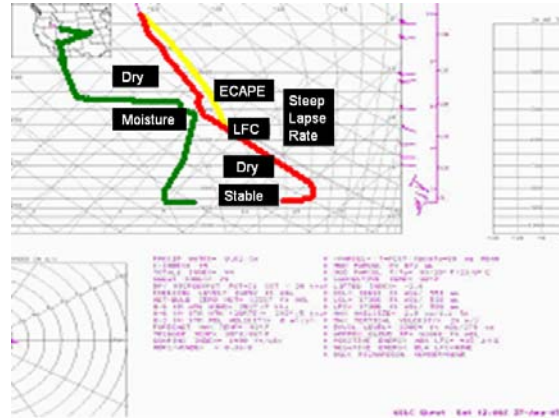


*Fig. 7. Skew T-logp plot for KSLC at 1200 UTC 27 August 2005. This sounding displayed the common profile observed during the significant elevated thunderstorm events. Dry and stable layers are depicted along with the moisture layer and resultant ECAPE (yellow line). Note the "hourglass" look.*

## 4. SIGNIFICANT EVENTS

### 4.1 September 8 to 9 1999

The basic synoptic pattern for this event was dominated by an upper level area of lower pressure situated in the eastern Pacific Ocean (Fig. 8) Figure 9 depicts a disorganized line of strong thunderstorms that developed ahead of the upper trough and extended from just south of Monterey Bay northward to the San Francisco Bay. Thunderstorms persistently developed south of Monterey Bay, over the Pacific Ocean, and then moved north across land. Surface observations and the NLDN indicated that the thunderstorms produced heavy rain and frequent cloud-to-ground lightning for several hours in major populated areas such as San Jose. Figure 10 depicts the several hundred strikes which occurred over the Pacific Ocean and coastal areas from 2000 UTC 8 September to 0000 UTC 9 September 1999. Nearly 5000 total lightning strikes were observed in this event.

The upper air sounding at Oakland (KOAK) for 0000 UTC 9 September was observed just prior to the main thunderstorm outbreak (Fig. 11). The sounding clearly depicted an elevated layer of instability above the stable marine boundary layer. The 900 to 600-mb lapse rate on the KOAK sounding, above the stable marine layer, was near
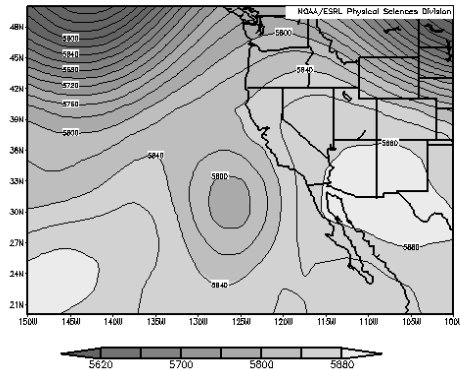
Fig. 8. 500-mb geopotential height daily mean composite reanalysis for 8 September 1999 (every 20 m).
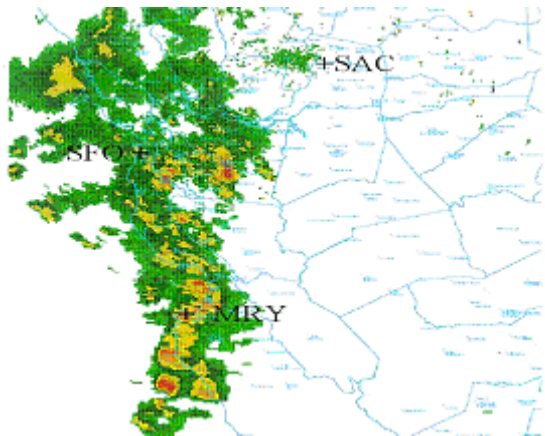


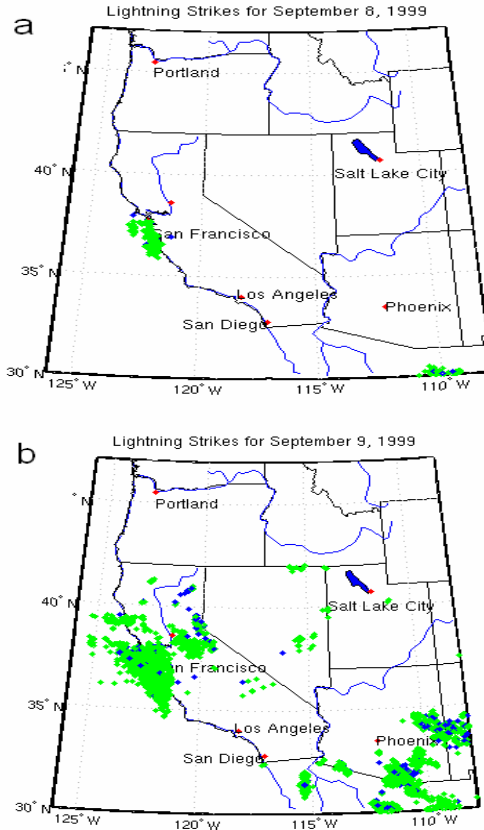Fig. 9. WSR-88D mosaic composite reflectivity at 0530 UTC 9 September 1999.



Fig. 10. NLDN plot for (a) 8 September and (b) 9 September 1999 (UTC). Green symbols indicate negative strikes and blue symbols are positive strikes. MATLAB used to display (appendix).
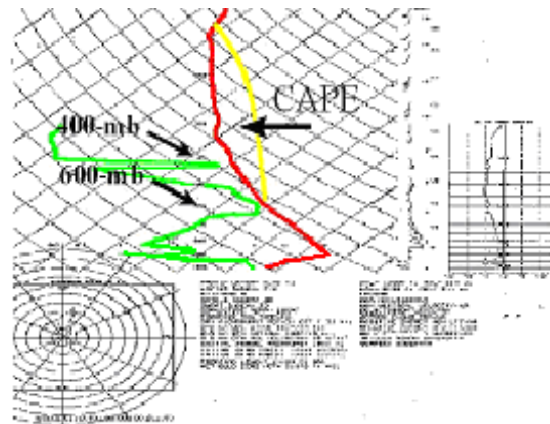


Fig. 11. Skew T-logp plot of observed temperature and dewpoint for KOAK at 0000 UTC 9 September 1999. ECAPE estimated using an elevated parcel.

dry adiabatic (10°Ckm$^{-1}$) which would indicate potential instability. The sounding depicted the moisture source for potential deep moist convection was in a layer between 650 and 500-mb and is similar to the so called "inverted-V" sounding (Bluestein 1993). This classic type of sounding has been documented as the Beebe "Type IV" (Bluestein 1993; Beebe 1955). Often this is not the level in the atmosphere across the western United States where a meteorologist would expect intense rain producing thunderstorms to form, but rather high-based thunderstorms producing infrequent lightning and virga or light precipitation. The KOAK sounding also resembles the Miller "Type I" sounding since the boundary layer has a stable layer below the region of low static stability (Bluestein 1993; Miller 1972). KOAK displayed a capped moist boundary layer and CIN. However, we will demonstrate that the boundary layer did not play a role in the formation of thunderstorms for this and many other events.

The findings in this study indicated the existence of significant subtropical moisture in the 650 to 450-mb layer was crucial. As an initial comparison to how well the numerical models forecast this event, Figure 12 is a forecast sounding valid at 1200 UTC 9 September 1999 for KOAK. The Eta sounding at KOAK, viewed in the Buffalo

Toolkit or BUFKIT (Mahoney and Niziol 1997, 2000), revealed that this 24-h forecast very closely resembled the observed sounding shown in Figure 13.
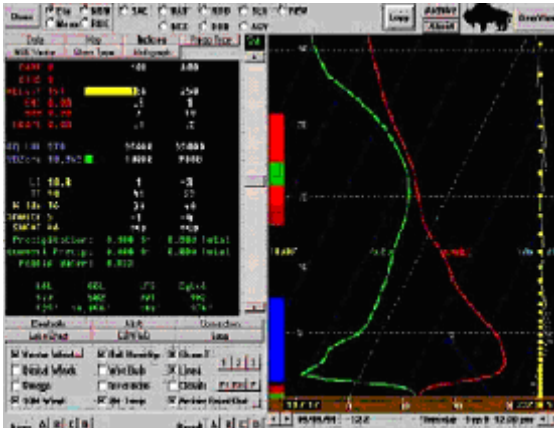


Fig. 12. BUFKIT KOAK profile from the 1200 UTC 8 September 1999 NAM forecast (formerly Eta) run valid at 1200 UTC 9 September 1999.
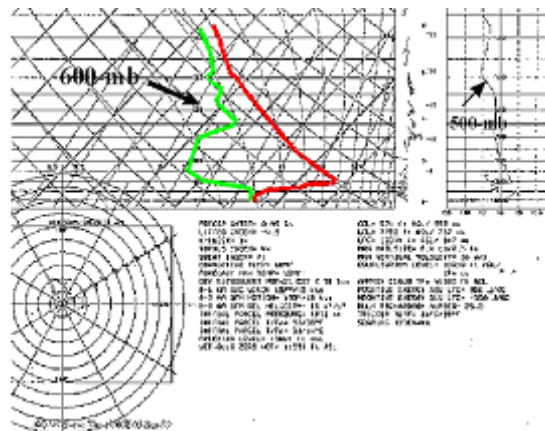


Fig. 13. Skew T-logp plot of observed temperature and dewpoint for KOAK at 1200 UTC 9 September 1999.

A Rapid Update Cycle (RUC) model sounding (Fig. 14) for a point selected at a location near San Jose (KSJC) depicted a profile very similar to the KOAK sounding in Figure 13. This had a most unstable (MU) convective available potential energy (CAPE) value of 1331 Jkg$^{-1}$ and a 500-mb lifted index (LI) of -6.5 °C. Above the marine layer this sounding clearly depicted a potentially unstable atmosphere conducive to strong thunderstorms if sufficient moisture and lift were also available. At 1200 UTC 9 September, the KOAK sounding (see Fig. 13) remarkably shows that there is little change in the low to mid-level temperature and moisture profiles that were observed at 0000 UTC (see Fig. 11). Precipitable water amounts had increased to almost 25 mm, while the 24-h change profile showed noticeable cooling above 550 mb. A deep dry layer was still present between the top of the marine inversion and 650 mb. Observed lapse rates were nearly dry adiabatic from 900 to 600-mb. Wind profiles continued to indicate a layer of southeasterly flow between the 700 and 500-mb levels (suggestive of a closed circulation), while there was an onshore flow (west) below 800 mb. The veering wind direction with height between the 800 and 700-mb levels is a possible indication of warm air advection. This would result in additional air mass lifting within this layer and supported steep lapse rates.

Water vapor imagery has always been a valuable tool for a weather forecaster, and is crucial for identifying pre-elevated thunderstorm environments. Surface data will often reveal few clues to the potential for elevated thunderstorms, since the moist convection can be initiated over cold water, valleys, or high terrain, and has no dependence on surface or boundary layer conditions. Figure 15 is a Geostationary Operational Environmental Satellite (GOES) water
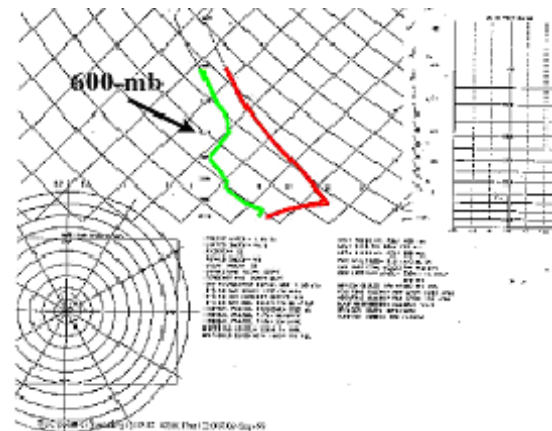


Fig. 14. RUC forecast sounding at a point location for San Jose CA at 1200 UTC 9 September 1999. This was similar to the observed KOAK profile. This sounding depicted CAPE of 1331Jkg$^{-1}$.

vapor image taken at 2200 UTC 8 September, which is near the time thunderstorms were first evident. This image depicted a circulation in the mid-troposphere which is approaching the West Coast. Very dry air had been advected into the upper low (orange and yellow color scale represents drier air), but closer examination indicated that slightly more moist air was being drawn to the northwest (within the southeast flow) ahead of the mid-level circulation. A time lapse of water vapor imagery (not shown) illustrated the air mass becoming closer to saturation as indicated by the darkening in the water vapor imagery on the California coast in Figure 15. Once the dynamics associated with the upper low interacted with the subtropical moisture surge, explosive deep moist convection was evident on satellite at 0300 UTC 9 September (Fig. 16).

The individual thunderstorms weakened as they were carried northward into an area of subsidence on the north side of the upper trough. Several hours later satellite imagery (not shown) depicted a weaker upper air system with a large area of anvil cirrus associated with the thunderstorms. The line of thunderstorms that was seen in the composite reflectivity image from Figure 9 remained intact and had moved inland, persisting over the San Francisco and Monterey Bays. The mid-level dry air, observed at 0000 UTC 9 September between 500 and 400 mb and above a moist layer around 600 mb (see Fig. 11), allowed for steeper environmental lapse rates since the dry air was cooled faster when it was lifted. The cooling, or steepening lapse rates, are evident on the 24-h temperature change scale on the right side of Figure 11. This cooling can also be attributed to cold air advection associated with a colder pool of air in the mid-tropospheric circulation.



Fig. 16. GOES-10 water vapor image at 0300 UTC 9 September 1999.

Using basic 500-mb geopotential height, omega and relative humidity model forecasts in plan view demonstrated how well the upper level forcing and saturation was predicted (Fig. 17). We have found that using the 500-mb layer or a defined mean layer (e.g., 600 to 450 mb) to be useful for diagnosing elevated moist convection, but it must be used in combination with forecast soundings. Assessing the depth of the elevated instability has been found to be more important than the amount of moisture and dynamic lift (i.e., omega) since the response in the atmosphere will be much greater for deeper instability. However, given deep layer instability, which is often present during the warm season, the introduction of moisture yields the larger ECAPE and the greatest potential for elevated convection.
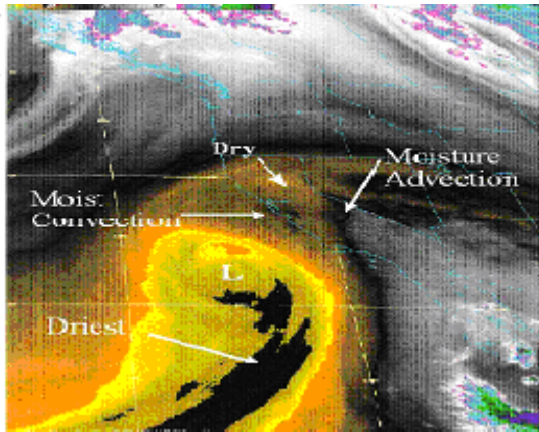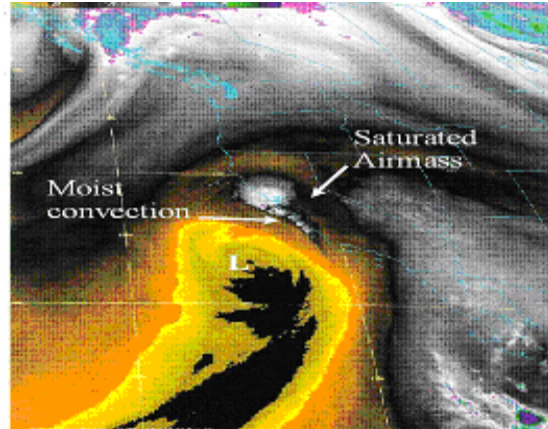


Fig. 15. GOES-10 water vapor image at 2200 UTC 8 September 1999.

The enhancements (-40°C or colder) seen in the far lower right side, and far upper portions of Figures 15 and 16, proved not to be relevant to this case. Since water vapor imagery is most sensitive to moisture near 400-mb, these enhancements are often by-products of deep moist convection or cyclogenesis, rather than indications of moisture advection below 500 mb. In other words, the important moisture source between 700 and 500 mb can be overlooked on the water vapor imagery, while the enhanced areas could be given too much consideration. In this case, careful examination of water vapor imagery did reveal the moisture advection between the 650 and 500-mb levels (see Figs. 15 and 16).
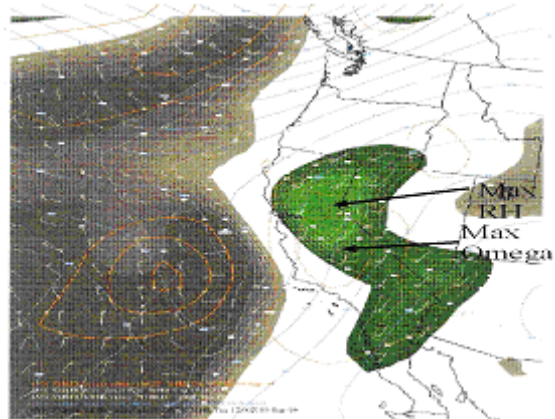


Fig. 17. GFS (formerly AVN) 36-h forecast of 500-mb geopotential height, omega and relative humidity (shaded) valid at 1200 UTC 9 September 1999.

### 4.2 September 24 to 25 2001

On 24-25 September 2001 the synoptic pattern (Fig. 18) was very similar to those in prior elevated thunderstorm studies (Tardy 2001) as well as the 8-9 September case presented in section 4.1. This included a mid-tropospheric closed low pressure system approaching the coast of California and a dry and stable air mass over central California (not shown). Ahead of this system upward vertical motion was being generated by differential positive vorticity and warm air advection processes. An upper-level jet stream maximum had moved directly over central California, east of the upper low. The southerly mid-level flow ahead of the storm was drawing subtropical moisture (higher precipitable water values) northward into California.
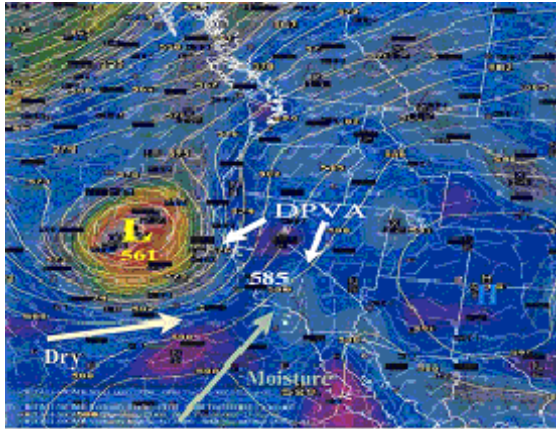
The 0000 UTC 25 September sounding from KOAK indicated a large quantity of elevated instability or ECAPE (Fig. 21). In addition, the dry air above 400 mb (see Fig. 21) would increase the environmental instability due to evaporative and adiabatic cooling as the upper-level air mass is lifted at the dry adiabatic lapse rate (faster rate of cooling than the moist rate). A RUC sounding for 2100 UTC, at a Sacramento (SAC) grid point, also indicated a conditionally unstable environment with calculated MUCAPE of 523 $Jkg^{-1}$ (Fig. 22). However, surface-based convection was not supported because of a very high LFC due to a dry deep boundary layer and insufficient low-level convergence. A surface analysis of CAPE at 2000 UTC indicated that there was no surface-based CAPE in the Central Valley of California (Sacramento location), but there was over the higher terrain (Fig. 23).



Fig. 18. NAM (formerly Eta) analysis at 0000 UTC 25 September 2001. Height lines every 30 m, half wind barbs every 2.5 ms$^{-1}$ and vorticity (shaded) every 2 1e5s$^{-1}$.
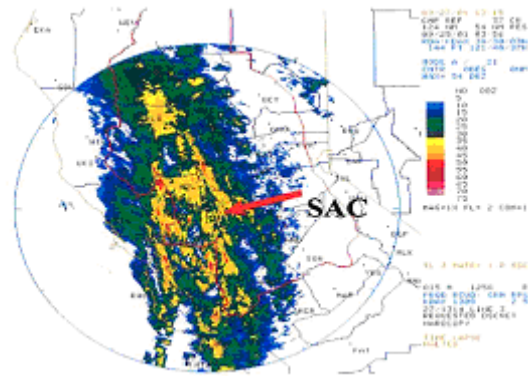


*Fig. 19. KDAX composite reflectivity image at 0356 UTC 25 September 2001.* SAC label denotes location of Sacramento.

On the east-northeast side of this upper low, the greatest low-level speed convergence and upper-level divergence produced large scale vertical ascent of the air mass. This was found to be the prime location for thunderstorm development. This finding is similar to a study by Colman (1990) which illustrated that the maximum frequency of elevated thunderstorms was near the inflection point. The inflection point is where the greatest divergence can occur on the east side of a trough due to strong ageostrophic compensation of the wind flow.

A line of intense thunderstorms developed along the west central coast of California and moved into the Sacramento (SAC) Valley (Fig. 19). These thunderstorms produced over 4000 lightning strikes as shown in the NLDN plots (Fig. 20). The lightning was most significant during the night hours.

Fig. 20. NLDN plot for (a) 24 and (b) 25) September 2001 (UTC). Green symbols indicate negative strikes and blue symbols are positive strikes. Sacramento is labeled for reference in 20a.

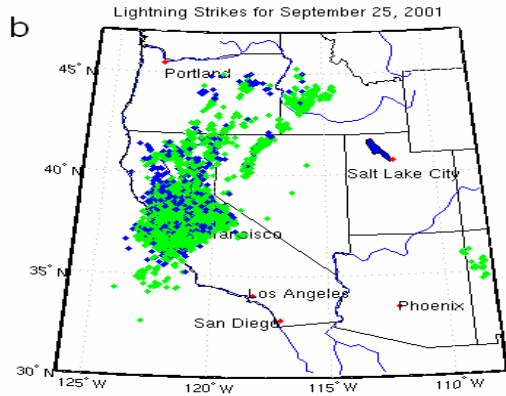In this case, the thunderstorms were not rooted in this KOAK stable layer. The marine layer observed at KOAK was not present over the Central Valley when the first thunderstorms developed, but rather a subsidence inversion (i.e., cap) existed which is common during the summer months. In addition, dry low to mid-levels of the Central Valley created an LFC that was not reachable for surface-based parcels (i.e., zero surface-based CAPE).
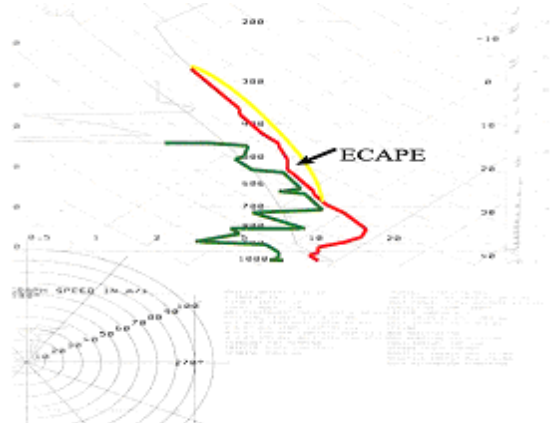


Fig. 21. Skew T-logp plot of observed temperature and dewpoint for KOAK at 0000 UTC 25 September 2001. Precipitable water had increased to 30.7 mm.

It is crucial to recognize that the instability (nearly dry adiabatic) is elevated over the inversion layers depicted in Figure 21. It was suggested by Colman (1990) that the decoupling could act to decrease the drag on the overriding air and may allow for more efficient convective overturning.
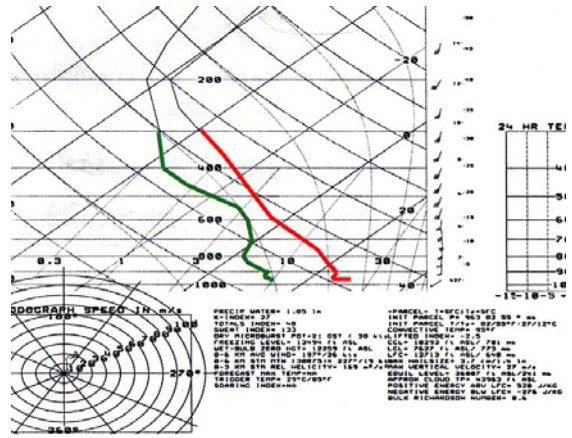


Fig. 22. RUC sounding at a point over Sacramento (SAC) for 2100 UTC 24 September 2001.

This study supports this theory since elevated thunderstorms have been observed when boundary layer conditions were dominated by marine, radiational, and subsidence inversions. However, the inversion layer was not a prerequisite to elevated thunderstorms but rather an inhibitor of surface-based mixing into the mid-troposphere. The first development of convective clouds, altocumulus castellanus, was depicted in a GOES-10 visible (.39 µ) image at 1800 UTC (Fig. 24).
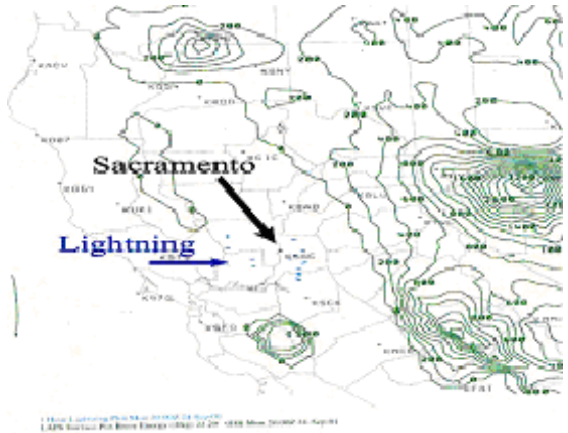


Fig. 23. Surface analysis of CAPE at 2000 UTC 24 September 2001. Contoured every 200 Jkg$^{-1}$. 1-h lightning strikes indicated by small blue lines. Sacramento located in the Central Valley.

The significance of these clouds is that they have been found to be precursors to elevated thunderstorms and indicative of mid-level moisture and instability (Corfidi and Schutlz 2006). At 2000 UTC infrared (IR) imagery indicated the thunderstorms had developed further northeast in the southern Sacramento Valley (not shown).

Fig. 24. GOES-10 visible image at 1800 UTC 24 September 2001. Altocumulus castellanus (ACC) and towering cumulus (TCU) noted east of the stratus cloud area.

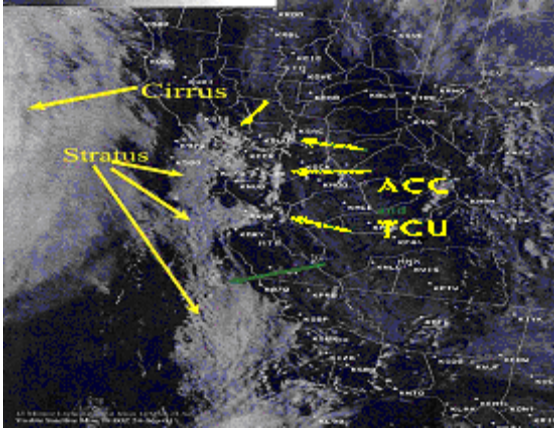The GOES-10 water vapor image at 2130 UTC gave subtle indications of significant moisture advection southeast of the mid-tropospheric low pressure area as seen with the brightening (cooling) due to synoptic layer lifting east of the system (Fig. 25). Although the cold frontal rain band was developing offshore in Figure 26, the moisture advection was most apparent on the Special Sensor Microwave/Imager (SSM/I) data which indicated the significant moisture plume having origins from the subtropics (Fig. 27). This rapid influx of moisture into the initially dry region was vital to the destabilization of the air mass. At 1200 UTC 24 September the observed precipitable water value at KOAK was only 8.9 mm (Fig. 28). The sounding twelve hours later revealed a large increase in moisture with a precipitable water value reaching 30.7 mm by 0000 UTC 25 September (see Fig. 21). A NAM forecast sounding from the 1200 UTC 24 September run and valid at 1200 UTC 25 September correlates well with the instability observed at Sacramento (Fig. 29)
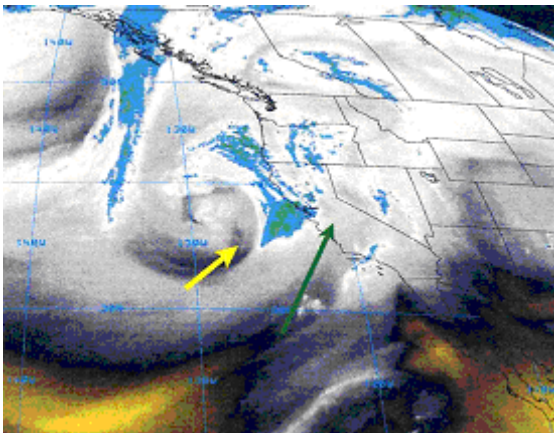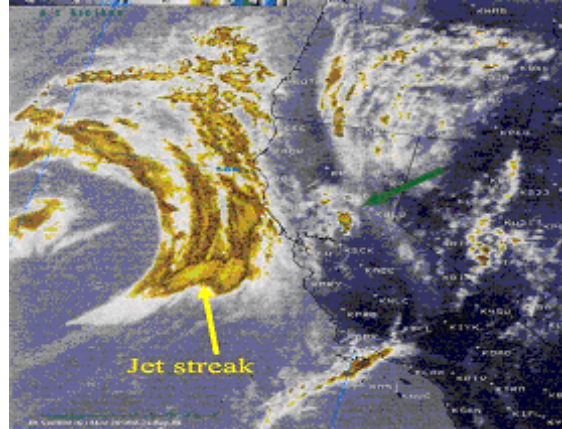


Fig. 26. GOES-10 10.7 μ image at 2000 UTC 24 September 2001.

The GOES-10 IR image also illustrated the location of an upper-level jet streak moving toward central California (see Fig. 26). North to south oriented enhanced cloudiness (cold cloud tops) perpendicular to this jet streak depicted the region of strongest mid to upper-level vertical motion on the east side of the mid-tropospheric system. In this region, an organized and intense area of thunderstorms developed just offshore and advected into the Sacramento Valley (see Fig. 19 ). The NLDN detected more than 500 cloud-to -ground strikes in the Central Valley and coastal hills between 0400 and 0500 UTC (not shown).



Fig. 27. SSM/I precipitable water plot at 0200 UTC 25 September 2001.

Over 200 lightning strikes per hour were detected from 2200 UTC 24 September through 1100 UTC 25 September from the coast to the Sierra Nevada (see Fig. 20). The peak hour of lightning activity was from 0200 to 0300 UTC when 702 strikes were recorded (mostly along the coast). The IR image at 0715 UTC 25 September depicted a large area of intense thunderstorms over the Central Valley and a well-defined upper-level diffluent pattern (Fig. 30).



Fig. 25. GOES-10 water vapor at 2130 UTC 24 September 2001.

Fig. 28. Skew T-logp plot of observed temperature and dewpoint for KOAK at 1200 UTC 24 September 2001.

This, and other elevated thunderstorm studies, have illustrated that despite the dry air on the KOAK sounding noted below 700 mb (see Fig. 21), thunderstorms can become strong enough to bring the low-levels of the atmosphere closer to saturation and produce significant rainfall even though the sub-cloud layer may initially be very dry. In this case, the Sacramento Valley received rainfall amounts ranging from 6 to 13 mm within a 1 to 2-h period, while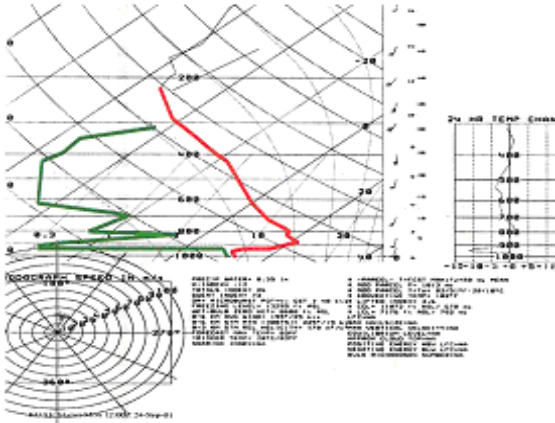 across the higher terrain amounts locally exceeded 25 mm. This amount of rainfall in such a short period is unusual for California during the warm season.
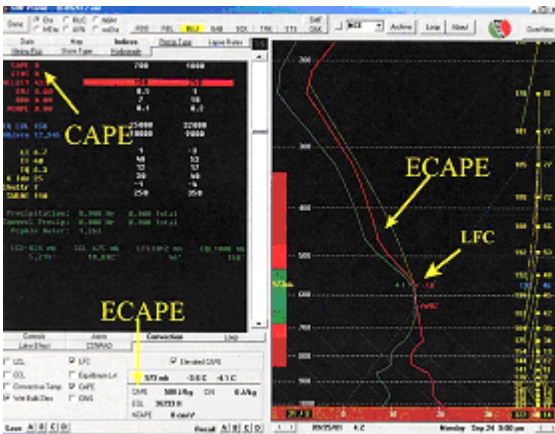


Fig. 29. BUFKIT KSMF profile from the 1200 UTC 24 September NAM (formerly Eta) run valid at 0400 UTC 25 September 2001. Forecast ECAPE (Jkg$^{-1}$) indicated on sounding.

### 4.3  September 3 2004

An organized band of elevated thunderstorms developed across the northwest deserts of Utah during the evening of 3 September 2004 (Fig. 31). A swath of lightning was observed across this region (Fig. 32). The thunderstorms initially developed above dry low level air with no surface-based or boundary layer CAPE (Fig. 33). The convection was intense for several hours as individual cells tracked across the Great Salt Lake and the northern Wasatch Front. The moist convection depicted an increase in intensity through the night hours (i.e., 0700 to 1300 UTC). Satellite imagery depicted the intense vertical motion that supported the development and long duration of the thunderstorms across northern Utah (Fig. 34).
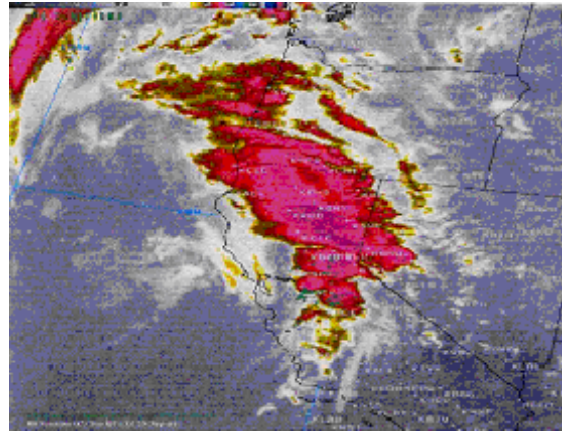


Fig. 30.  GOES-10 10.7 µ image at 0715 UTC 25 September 2001.

By the early morning hours on 3 September the thunderstorms continued and were embedded in a large area of stratiform rain. The 1200 UTC KSLC sounding in Figure 35 depicted the moist low levels with modest ECAPE present in the mid and upper-levels. This sounding was likely launched into the remaining convection but had little cooling aloft and zero surface-based CAPE or MUCAPE.

This event was similar to the others in this paper but occurred across the deserts of northwest Utah after the boundary layer was originally very dry and well-mixed. The importance of dynamic lift acting on sufficiently deep ECAPE demonstrated heavy rainfall (implied strong upward motion) overcoming initially very dry subcloud layers. Other events in this study depicted similar bands of elevated thunderstorms in northern Utah which were not influenced by the deserts, lakes, mountains or insulation (e.g., 25 August 2006 in Table 1 and Figure 36). The convection trained along a mid-level boundary and was persistent for several hours. This pattern is common during the cold season but the response of the atmosphere is typically less (exception would be slantwise convection) due to higher stability. Numerical model performance in most of the elevated convection events was good for moisture fields but poor for quantitative precipitation forecasts (QPF). However, in case 3 and more recent events the model QPF (e.g., NAM-WRF) performance was better.
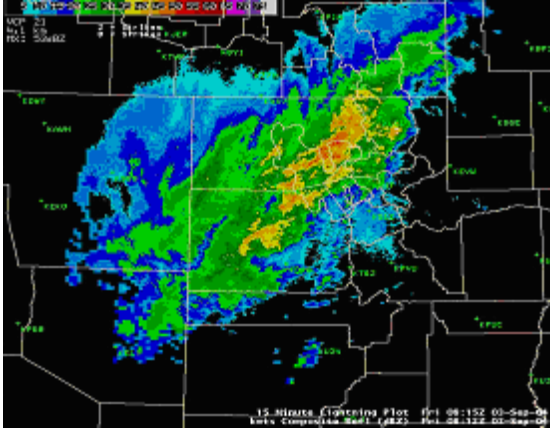
Fig. 31. KMTX composite reflectivity at 0815 UTC 3 September 2004.
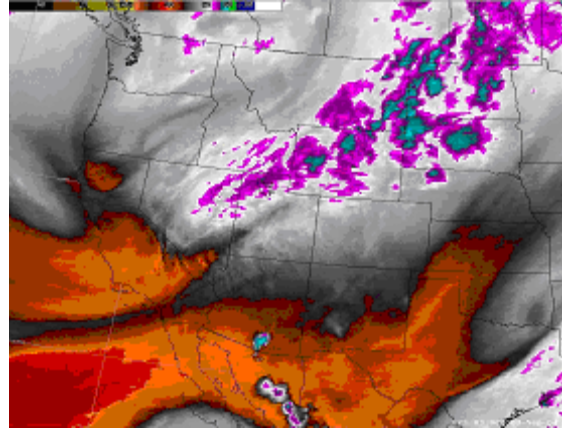


Fig. 34. GOES-10 water vapor image at 0300 UTC 3 September 2004.
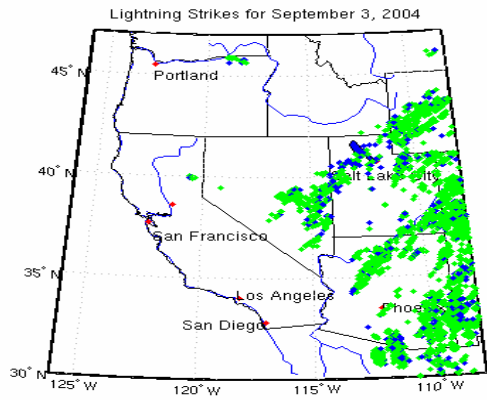


Fig. 32. NLDN plot for 3 September 2004 (UTC). Green symbols indicate negative strikes and blue symbols are positive strikes.
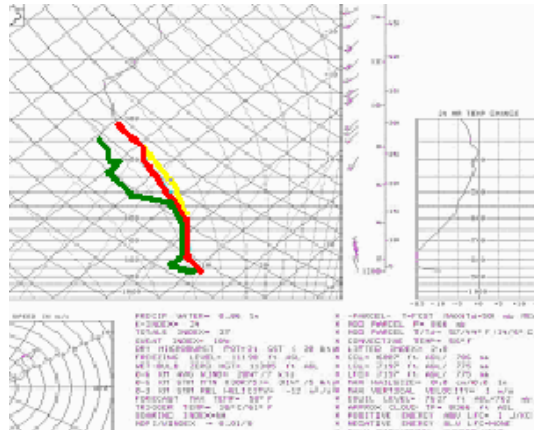


Fig. 35. As in Fig. 33 for 1200 UTC 3 September. Zero CAPE in the lowest 300 mb.
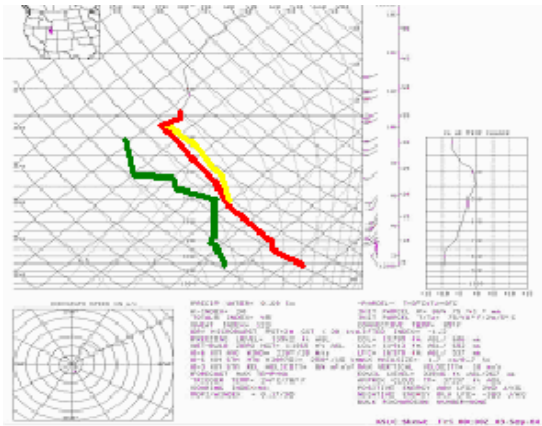


Fig. 33. Skew T-logp plot of observed temperature and dewpoint for KSLC at 0000 UTC 3 September 2004. Note the two dry layers. Yellow line is ECAPE
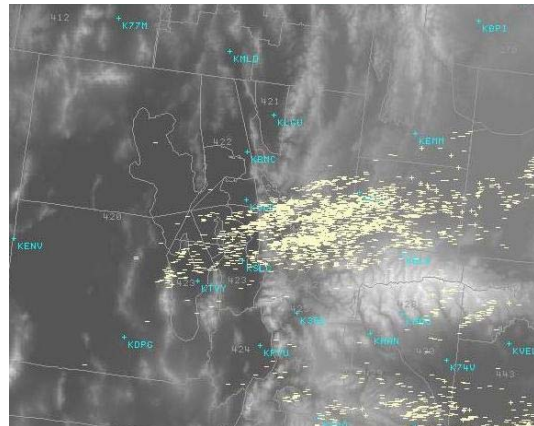


Fig. 36. 24-h NLDN plot of lightning strikes ending at 1100 UTC 25 August 2006 across northern Utah. Image is terrain (higher terrain in white).

## 5. FORECASTING APPLICATIONS AND DISCUSSIONS

The elevated thunderstorm events in this study were likely very difficult for forecasters to anticipate because they were not rooted in the boundary layer. Therefore, it was not uncommon for a significant lightning outbreak to have occurred with little or no thunderstorms forecast or a decreasing trend anticipated. The purpose of this preprint was to highlight the general findings and not discuss numerous events. These findings identify the processes and mechanisms that led to elevated thunderstorm outbreaks. It is hoped that these results will able forecasters to better understand and predict such events in the future.

In order for elevated thunderstorms to develop there needs to be sufficient moisture above the boundary layer. Secondly, adequate instability must be present above the boundary layer. Lastly, lift is required to effectively lower or allow air parcels to reach the LFC (destabilization). One way to assess the magnitude of the lift is to examine geopotential height fields with omega and differential positive vorticity advection at the 500-mb level or in a defined layer encompassing this pressure level. The 500 and 600-mb levels were found to be useful in diagnosing the moisture and vertical velocity maximums (omega) that led to the thunderstorm development in this study because the elevated moisture and instability were often greatest in this layer.

Warm air advection between the 850 and 700-mb level will also contribute to the upward vertical motion. The majority of the elevated thunderstorm cases studied by Colman (1990) exhibited significant warm air advection at 850 mb. Upper-level low pressure areas and short-wave troughs associated with these mid-tropospheric systems can often be viewed on water vapor imagery (see Figs. 15 and 16) and have been found to be forecast reasonably well by numerical models. In addition to the requirement of mid-level upward vertical motions, upper level divergence played an important role in the location and strength of the most organized thunderstorms. The importance of upper divergence for thunderstorm development is not a new finding, but it does demonstrate how significant jet dynamics can be when subtropical moisture, elevated instability and synoptic scale lift interact across the western United States.

The combination of dynamics and sufficiently deep layer ECAPE have proven to produce elevated thunderstorms with the intensity, duration and areal coverage as those more commonly associated with surface-based CAPE. It is not suggested that the dynamics associated with short-wave troughs produce thunderstorms, but rather

the environment experiences saturation and destabilization through synoptic motions which then allow random air parcels to realize the potential instability on the mesoscale. Given high potential instability in the atmosphere small-scale and subtle short-wave troughs or vorticity maximums were observed in satellite and high resolution model data (e.g., NAM-WRF) to be associated with elevated moist convection.

Water vapor imagery will also detect important moisture advection patterns and air mass layer lifting prior to condensation (cooling signatures). The most effective way to verify the presence of deep moisture and instability is to view the available upper-air data, satellite microwave imagery and soundings, and model-derived soundings. Examples of a model sounding that accurately predicted the elevated instability and moisture is demonstrated using the BUFKIT software in Figures 12 and 29. The use of model soundings has proven to be vital for determining the depth of elevated instability and therefore useful in forecasting elevated thunderstorms. Traditional methods for assessing the potential for boundary layer convection such as surface heating, boundary and terrain interaction, outflow cool pools, and the availability of low to mid-level moisture (including surface dewpoints) were not useful for forecasting elevated moist convection and may hinder the forecast process based on this study.

## 6. GENERAL CONCLUSIONS

It has been demonstrated in this climatological study, and in the entire series (Tardy 2001, 2002), that the synoptic scale vertical motion in a rapidly moistening and destabilizing air mass ahead of upper-level low pressure systems, and individual short-wave troughs can result in explosive thunderstorm development. Elevated thunderstorms with no surface-based CAPE have been observed along the coastal areas, over the Pacific Ocean, in the Central Valley of California, and across the rest of the valleys, deserts and mountains in the western United States with similar characteristics to those in this study. Elevated thunderstorms can bring heavy rain to parts of California, which typically have very little rainfall during the summer months. More significantly, these thunderstorms can produce large numbers of cloud-to-ground lightning strikes that can ignite forest fires in areas of severe dry ground conditions which are common in the summer months across the western United States.

The process for developing elevated thunderstorms was explained as synoptic scale vertical motion taking the air mass closer to saturation and effectively lowering the LFC (destabilization) thus allowing random air parcels to

become buoyant and develop into deep cumulus and thunderstorms. A sounding with a steep lapse rate and the process of rapid modification to the air mass (e.g., moisture advection), like those illustrated in Figures 21 and 28, are not rare for the western United States. Elevated thunderstorms need to be considered in this type of environment. There is some evidence from other cases that pre-existing mid-tropospheric outflow boundaries from prior diurnal thunderstorms can enhance or focus the thunderstorms (not shown). However, satellite and radar data in this climatological database suggested that this is not a prerequisite.

The location of initial thunderstorm development can be random, with no dependence on terrain or boundary layer conditions. The first thunderstorm development is often in the region of synoptic scale vertical motion and upper-level divergence that had interacted with a significant subtropical moisture surge or moisture already present. The most organized thunderstorms, and thus the heaviest rainfall, occurred in the region of strongest dynamics and greatest mid-level vertical motions with deep elevated instability (ECAPE) and were independent of dry or stable boundary layer conditions.

Examination of water vapor imagery is important for the detection of air mass layer lifting and subsequent moistening prior to cloud and thunderstorm development. The IR and visible channels can be very useful for detecting altocumulus castellanus (mid-level moisture and instability) which is often a precursor to elevated thunderstorms. Focusing on the enhanced cold cloud tops on the water vapor will often be misleading since this is typically the product of existing or prior thunderstorm anvils.

Numerical models have demonstrated skill in predicting moisture fields and accurate thermal profiles of the atmosphere which produce elevated convection. The use of model layer or single-level omega, relative humidity, and precipitable water along with forecast soundings were shown to be a reliable tool for anticipating conditions favorable for elevated thunderstorms. Model QPF and the use of plan view model data alone can be misleading. In the short term, model, satellite derived, and observed soundings can indicate elevated instability and moisture that are present or forecast to occur. The single most important finding in this study is that forecasters should not use surface-based or boundary layer data, terrain, insulation, and low level inversions or dry layers when diagnosing the potential for elevated convection. In practice this has proven to be difficult.

It is hoped that the findings from this paper will aid the understanding and enhance the ability for forecasters to better predict elevated thunderstorm events that are often unexpected or severely underforecast.

## 7. REFERENCES

Beebe, R. G., 1955: Types of Air Masses in Which Tornadoes Occur. Bull. Amer. Meteor. Soc., 36, 349-350.

Bluestein, H. B., 1993: Synoptic-Dynamic Meteorology in Midlatitudes Vol. II Observations and Theory of Weather Systems. Oxford University Press, 2, 444-455.

Colman, B. R., 1990: Thunderstorms above Frontal Surfaces in Environments without Positive CAPE. Part I: A Climatology. *Mon. Wea. Rev.*, 118, 1103-1122.

Colman, B. R., 1990: Thunderstorms above Frontal Surfaces in Environments without Positive CAPE. Part II: Organization and Instability Mechanisms. *Mon. Wea. Rev.*,118, 1123-1144.

Corfidi, S.F. and S.J. and D. M. Schultz, 2006: Toward a better understanding of elevated convection. Preprints, *23rd Conf. Severe Local Storms*, St. Louis, MO, Amer. Meteor. Soc. [CD-ROM]

Horgan, K. L., D. M. Schultz, J. E. Hales Jr., S. F. Corfidi, and R. H. Johns, 2006: A five-year climatology of elevated severe convective storms in the United States east of the Rocky Mountains. Submitted to Wea. Forecasting.

Mahoney, E. A., cited 2000: BUFKIT Documentation [Available on-line from http://www.nws.noaa.gov/er/buf/bufkit/bufkitd ocs.html].

Mahoney, E. A., and T. A. Niziol, 1997: BUFKIT: A software application toolkit for predicting lake-effect snow. Preprints, *13th Intl. Conf. on Interactive Information and Processing Systems for Meteorology, Oceanography, and Hydrology*, Long Beach, CA, Amer. Meteor. Soc., 388-391.

Miller, R. C, 1972: Notes on Analysis and Severe

Storms Forecasting Procedures of the Air Force Global Weather Central. Tech. Rep. 200 (Rev. 1975). U.S. Air Force, Air Weather Service.

Tardy, A. O., 2002: 24-25 September 2001 event in the Sacramento Valley. Western Region Technical Attachment No. 02-15.

Tardy, A. O., 2001: Forecasting Applications for Elevated Thunderstorm in California, Part 1:The 8 September 1999 Outbreak. Western Region Technical Attachment No. 01-09.

Tardy, A. O., 2001: Persistent Nocturnal Thunderstorms over Central California in August, Part 2. Western Region Technical Attachment No. 01-12.

Tardy, A. O., 2001: Elevated Thunderstorms over the San Joaquin Valley, Part 3: The 22 September 1999 Nocturnal Event. Western Region Technical Attachment No. 02-03

**8. APPENDIX**

**LINKS**

http://www.cdc.noaa.gov/Composites/Day/   (CDC)

http://www.wdtb.noaa.gov/tools/BUFKIT/index.html (BUFKIT)

http://www.ncrs.fs.fed.us/4401/focus/climatology/firewx/ (Fire weather)

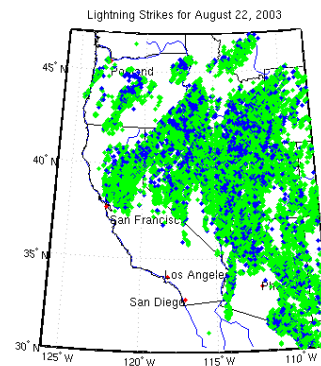http://www-ccs.ucsd.edu/matlab/techdoc/ umg/umg.html  (MATLAB)

http://www.mathworks.com/products/mapping/ (MathWorks toolbox)



Example of lightning plot using MATLAB for the 22-23 August 2003 event.

Table 1.  List of time (UTC) and location for events used in this study.  Lightning from the NLDN was detected unless otherwise noted.  Notes were included which may further support the study (e.g., location and time of day).

| Date | Location | Lightning | Notes |
|---|---|---|---|
| 9-10 Aug 1999 | Northern CA | | grass fires night |
| 23 Aug 1999 | Northern CA | | valley and night |
| 26 Aug 1999 | CA | | ocean and night |
| 27 Aug 1999 | Central CA | | valley |
| 8-9 Sep 1999 | Central CA | near 5,000 | Big Sur Fire |
| 22 Sep 1999 | Central CA | | Tire Fire |
| 14 Oct 1999 | CA, OR | | ocean and eve |
| 10 Jul 2000 | Central CA | | grass fire and night |
| 2 Aug 2000 | Southern CA, NV | | ocean and night |
| 3 Aug 2000 | Central CA | | mountains and night |
| 7 Aug 2000 | Northern CA | | |
| 9 Aug 2000 | Northern CA | | early AM |
| 10 Aug 2000 | Northern CA | | coast and night |
| 1 Sep 2000 | Central CA | | rain valley crops |
| 4 Oct 2000 | Southern CA | | |
| 6 Dec 2000 | CA | | ocean and night |
| 22 Mar 2001 | CA | | night |
| 12 May 2001 | Southern CA | | valley |
| 3-4 Jul 2001 | Central CA | | |
| 10 Jul 2001 | Northern CA | | valley, early AM |
| 11 Jul 2001 | Northern CA | | valley and night |
| 14 Jul 2001 | Central CA | | |
| 24-25 Jul 2001 | Central CA | | |
| 7 Aug 2001 | Southern CA | | |
| 8 Aug 2001 | Central CA | | |
| 9 Aug 2001 | Northern CA | none detected | ACC clouds |
| 12 Aug 2001 | NV | | night |
| 4 Sep  2001 | Southern CA | | |
| 10 Sep  2001 | Northern CA | | |
| 12 Sep  2001 | Northern CA | | night |
| 15 Sep 2001 | Northern CA, OR | | coast and night |
| 25 Sep 2001 | Central CA | near 4,000 | valley and night |
| 15 Feb 2002 | Northern CA | none detected | |
| 23 Feb 2002 | WA, OR | | night |
| 28 Mar 2002 | Southern CA | | afternoon |
| 25 Apr 2002 | Central CA | | valley |
| 26 Apr 2002 | Central CA | | over stratus |
| 31 May 2002 | Southern CA | | |
| 1 Jun 2002 | Central CA | | valley and night |
| 14 Jun 2002 | WA | | coast |
| 3 Jul 2002 | Southern NV | | valley and night |
| 12 Jul 2002 | Central CA | | |
| 13 Jul 2002 | OR | | Biscuit Fire, day |
| 14 Jul 2002 | Southern NV | | |
| 21-22 Jul 2002 | Central CA | | |
| 5-6 Sep 2002 | Southern CA, NV | | |
| 7 Sep 2002 | Southern CA, NV | | early AM |
| 27 Sep 2002 | Southern CA | | coast, afternoon |
| 29 Sep 2002 | Southern NV | | |
| 17 Oct 2002 | Southern NV | | |
| 29 Nov 2002 | Southern CA | | ocean |
| 30 Nov 2002 | Southern NV | | |
| 23 Jul 2003 | Central CA | | |
| 24 Jul 2003 | Central CA | | coast and ocean |
| 25 Jul 2003 | Central CA | | |
| 1-2 Aug 2003 | Northern CA | 1,700 | night and early AM |
| 3 Aug 2003 | Northern CA | | |
| 7 Aug 2003 | OR | | |
| 15 Aug 2003 | OR | | over ocean |
| 21 Aug 2003 | Southern CA | | |
| 22 Aug 2003 | Northern CA | 4,230 | day and night |
| 26 Aug 2003 | Central CA | | coast and valley |
| 31 Aug  2003 | Central CA | | |
| 3 Sep 2003 | Central CA | | |
| 5 Sep 2003 | Northern CA | | coast |

| Date | Location | | Notes |
|---|---|---|---|
| 4 Jun 2004 | UT | | |
| 14 Jul 2004 | UT | | |
| 3-4 Sep 2004 | Northern UT | | heavy rain, night |
| 19 Sep 2004 | Northern UT | | |
| 6 May 2005 | UT | | |
| 30 May 2005 | Northern UT | | 1 in hail |
| 16 Oct 2005 | UT | | |
| 23 Jul 2005 | Central UT | | |
| 25 Jul 2005 | Northern UT | | |
| 19 Aug 2005 | Southern UT | | ½-in hail AM flood |
| 27 Aug 2005 | Northern UT | | |
| 26 Sep 2005 | Southern CA | | |
| 27 Sep 2005 | Central UT | | |
| 22 May 2006 | Northern UT | | |
| 3 Jun 2006 | Northern UT | | |
| 20 Aug 2006 | Central UT | | night |
| 22 Aug 2006 | Northern UT | | night |
| 25 Aug 2006 | Northern UT | 2,030 | night |
| 26 Aug 2006 | Northern UT | | night |
| 2 Sep 2006 | Southern UT | | early AM |
| 3 Oct 2006 | Southern UT | | |